Electronic Supplemental Information

A. Bioclimatic and habitat variables description

We used a set of moderately high-resolution climate and satellite remote sensing variables to characterize the habitat differences among our sampling areas. Variables were re-aggregated from their native resolutions to 5 km resolution.

1-Bioclimatic variables

We used 11 bioclimatic layers from the WorldClim database (Hijmans *et al*. 2005) which are 50-year averages (1950-2000) of annual means, seasonal extremes and degrees of seasonality in temperature and precipitation, and represent biologically meaningful variables for characterizing species range (Nix 1986; Sehgal *et al*. 2011):

(http://biogeo.berkeley.edu/worldclim/bioclim.htm)

BIO1 = Annual Mean Temperature

BIO2 = Mean Diurnal Range (Mean of monthly (max temp - min temp))

BIO4 = Temperature Seasonality (standard deviation *100)

BIO5 = Max Temperature of Warmest Month

BIO6 = Min Temperature of Coldest Month

BIO12 = Annual Precipitation

BIO15 = Precipitation Seasonality (Coefficient of Variation)

BIO16 = Precipitation of Wettest Quarter

BIO17 = Precipitation of Driest Quarter

BIO18 = Precipitation of Warmest Quarter

BIO19 = Precipitation of Coldest Quarter

2- Altitude

From the Shuttle Radar Topography Mission (SRTM), we acquired elevation data, with mean altitude and standard deviation as variables.

3- Surface moisture and canopy roughness

From QuikScat (QSCAT; http://www.scp.byu.edu/data/Quikscat/SIRv2/qush/World_regions.htm), we obtained monthly raw backscatter measurements that capture attributes related to surface moisture and canopy roughness (Long *et al.* 2001):

a) Qscat Mean: Annual mean Radar Backscatter of year 2001 (*for spatial distribution of surface moisture and roughness (forest structure*)); less negative means higher backscatter.

b) Qscat STD: Annual stdev of Radar Backscatter of year 2001 (*for spatial distribution of seasonality in surface moisture and roughness (forest structure*))

Unit: Decibel

4- Normalized Difference Vegetation Index

We used two NDVI (Normalized Difference Vegetation Indices; based on monthly files from the year 2001 of MODIS Data (1km resolution)):

a) NDVI max: Annual maximum NDVI (*for spatial distribution of vegetation density*)

b) NDVI range: Annual range NDVI (max-min; *for spatial distribution of seasonal vegetation activity*).

5- Percent Tree Cover

We used the vegetation continuous field (Hansen *et al*. 2002) product from MODIS (https://lpdaac.usgs.gov/lpdaac/products/modis_overview) as a measure of the percentage of tree cover in 2001.

B. Spatial autocorrelation analysis

Spatial autocorrelation statistics measure the effect of proximity of sampling sites on the variable of interest measured at those sites. This effect could either be positive, where nearby sites are more similar to each other than expected by chance, or negative, where nearby sites are more divergent than expected by chance. To determine whether spatial autocorrelation influenced the prevalence of *Plasmodium* parasites among our three main habitats, we calculated Moran's I (Moran 1950) using the *spdep* package (Bivand *et al*. 2009) in the R framework (R Development Core Team 2004). In addition we computed the autocorrelation coefficient *r* (Peakall *et al*. 2003) in Genalex (Peakall & Smouse 2006) to determine potential autocorrelation within habitat types. Distance classes were set to be at 50km intervals. We ran 999 iterative permutations and 1000 bootstrap replicates to estimate the autocorrelation coefficient *r* and to determine 95% confidence intervals for both the randomization of spatial relationships and subsampling of the dataset, respectively (Peakall & Smouse 2006). Across all habitat types, we observed no evidence of spatial autocorrelation in prevalence of *Plasmodium* (Moran's I = -0.011, $p = 0.8567$). Spatial autocorrelation in prevalence of diseases across broad geographic space might be expected, particularly given how distant our sampled habitats were from one another.

To ensure that our observed prevalence values within each of the three habitats were not reflective of pseudo-replication, we also tested for spatial autocorrelation within each of the three habitats separately. Within habitat types there was no indication of spatial autocorrelation in parasite prevalence, except for *Plasmodium* in fynbos at the distance class of 550 km (Fig. S2). We concluded that spatial autocorrelation is virtually absent in our dataset, and as it would not affect subsequent analyses, we did not consider further corrections.

C. Randomization protocol to test host-parasite assembly rule

The host-parasite assembly rule was investigated using an *ad hoc* randomization test. Based on the prevalence of parasites in each habitat (regardless of host species), the abundance of birds of all species (estimated by sample sizes), and assuming that host-parasite associations are random, a theoretical distribution (based on 10,000 iterations) of the number of species infected by each lineage in each habitat was constructed (= null model). Actual numbers of infected species were then compared to these expectations.

1. Randomization protocol

In each habitat, the abundance of each host species i was assumed to be proportional to the sample size for the species (N_i). The global prevalence of each *Plasmodium* lineage j in the habitat was assumed proportional to the number of individual hosts (of any species) infected by j ($=I_j$). N was the overall host sample size ($N=\Sigma N_i$).

For each *Plasmodium* lineage j for which I_j was equal to or greater than five, the following protocol was applied:

a. A host species i was randomly drawn.

b. A random number x was drawn from a uniform distribution [0, 1].

c. The species i was considered infected by j if $x<N_i/N$.

d. Operations (a) to (c) were repeated I_j times.

e. The number of host species infected by j was recorded.

f. Operations (a)-(e) were repeated 10,000 times and a distribution of the number of host species infected by all *Plasmodium* lineages was computed.

This protocol was separately applied to the three habitats.

2. Test

A one-sided P-value was computed by comparing the above null distributions with actual numbers of host species infected by each *Plasmodium* lineage in each habitat. P-values were then corrected by Bonferroni method multiplying the raw P-value by the overall number of tests (i.e., summing the tests conducted for the three habitats).

3. Results

For a given habitat, randomization tests were conducted only on *Plasmodium* lineages with five infected hosts or more, which yielded 16 separate tests (11 for lowland, 2 for highland and 3 for fynbos). Results indicated that host-parasite associations were not random for ten cases out of eleven for the lowland rainforest habitat (7 remain significant after Bonferroni correction). No significant departure from the null model was found for the two other habitats (however, as I_j values were smaller in fynbos and

highland, we could not exclude that this result is due to a lack of statistical power in these habitats). Detailed results are presented in Tables 1a, 1b and 1c3 below.

Table 1a. Comparisons of the actual numbers of infected species in the lowland rainforest habitat with the null distribution resulting from random association between individual hosts and parasites. P-values were computed as the probabilities that the number of infected species was equal to or smaller than the observed number under the assumption that the null model was true.

Plasmodium lineage	pv1	pv12	pv13	pv15	pv17	pv2	pv3	pv5	pv8	pv9	wa19
Number of individuals infected	23	5	8	24	35	10	22	5	6	11	12
Actual number of species infected	1	2	1	2	1	1	3	1	1	1	1
P-value	<0.0001	ns	0.0009	0.0005	<0.0001	0.0003	0.0247	0.0144	0.0043	<0.0001	<0.0001
Corrected P-value	<0.0016	ns	0.0144	0.008	<0.0016	0.0048	ns	ns	ns	<0.0016	<0.0016

Table 1b. Comparisons of the actual numbers of infected species in the highland habitat with the null distribution resulting from random association between individual hosts and parasites. P-values were computed as the probabilities that the number of infected species was equal to or smaller than the observed number under the assumption that the null model was true.

Plasmodium lineage	pv12	pv38
Number of individuals infected	27	5
Actual number of species infected	8	2
P-value	ns	ns
Corrected P-value	ns	ns

Table 1c. Comparisons of the actual numbers of infected species in the fynbos habitat with the null distribution resulting from random association between individual hosts and parasites. P-values were computed as the probabilities that the number of infected species was equal to or smaller than the observed number under the assumption that the null model was true.

Plasmodium lineage	p15	p16	pv41
Number of individuals infected	8	20	6
Actual number of species infected	3	4	2
P-value	ns	0.025	0.03
Corrected P-value	ns	ns	ns

D- Ancestral State Reconstructions and Trait Analyses

We estimated trait evolution (specifically, whether a parasite lineage was a specialist or a generalist) using the BayesTraits computer package (Pagel 1999). While specialist and generalist strategies can be considered extremes along a continuum of possible parasite strategies, we treated these two states as discrete characters as defined by the S_{TD} host index of each parasite lineage, mainly to understand difference in rate changes between these character states. To assess the sensitivity of this categorization, we tested several cutoff values used to distinguish specialist and generalist parasites, with highly concordant reconstructions for each (results not shown). A final cutoff value for established lineages corresponding to an S_{TD} value of 9: parasite lineages with values equal to or higher than this were considered generalists, whereas lineages with values below this were considered specialists. The cutoff value 9 represents a parasite that can infect more than 9 species and at least two families. Parasites that can infect several species from the same family are relatively common, and remain family specific;

however parasites that can infect different species from different families are considered as broad generalists (Krizanaskiene *et al.* 2006; Hellgren *et al*. 2009; Beadell *et al*. 2009). The value 9 is therefore a cutoff that is biologically appropriate.

Transitions between evolutionary strategies (specialist vs. generalist) were estimated across 2000 trees used to construct our consensus tree, using Bayes Multistate (Pagel & Meade 2006), under a maximum likelihood framework. Likelihood ratio scores were compared between a model that forced rates between evolutionary strategies to be equal, to a model with no constraints. The model with no constraints had a likelihood score more than two likelihood units (Lh = -16.359) greater than the constrained model (Lh = -21.810), suggesting that a two-rate model better fit our available data.

Ancestor states were reconstructed using the Addnode command in BayesTraits under a maximum likelihood framework, again treating evolutionary strategies as discrete character changes. For each node on our consensus tree, we calculated the proportion of the likelihood associated with each character state (generalist or specialist, Fig. 1).

References

Beadell JS, Covas R, Gebhard C, Ishtiaq F, Melo M, Schmidt BK, Perkins S, Graves GR, Fleischer R (2009) Host associations and evolutionary relationships of avian blood parasites from West Africa. *International Journal of Parasitology,* **39**, 257-266.

Bivand R, Muller WG, Reder M (2009) Power calculations for global and local Moran's. *Computational Statistics and Data Analysis*, **53**, 2859-2872.

Hansen MC, DeFries RS, Townshend JRG, Sohlberg R, Dimiceli C, Carroll M (2002) Towards an operational MODIS continuous field of percent tree cover algorithm: examples using AVHRR and MODIS data. *Remote Sensing of Environment,* **83**, 303-319.

Hellgren O, Perez-Tris J, Bensch S (2009) A jack-of-all-trades and still a master of some: prevalence and host range in avian malaria and related blood parasites. *Ecology,* **90**, 2840-2849.

Hijmans RJ, Cameron SE, Parra JL, Jones PG, Jarvis A (2005) Very high resolution interpolated climate surfaces for global land areas. *International Journal of Climatology,* **25**, 1965-1978.

Krizanauskiene A, Hellgren O, Kosarev V, Sokolov L, Bensch S, Valkiunas G (2006) Variation in host specificity between species of avian hemosporidian parasites: evidence from parasite morphology and cytochrome B gene sequences. *Journal of Parasitology*, **92**, 1319-1324.

Long DG, Drinkwater MR, Holt B, Saatchi S, Bertoia C (2001) Global Ice and Land Climate Studies Using Scatterometer Image Data. *EOS Transactions AGU,* **82**, 503.

Moran PAP (1950) Notes on Continuous Stochastic Phenomena. *Biometrika*, **37**, 17–33.

Nix H (1986) *A biogeographic analysis of Australian elapid snakes.* Atlas of Elapid Snakes of Australia. Australian Government Publishing Service.

Pagel M (1999) The maximum likelihood approach to reconstructing ancestral character states of discrete characters on phylogenies. *Systematic Biology*, **48**, 612–622.

Pagel M, Meade A (2006) Bayesian analysis of correlated evolution of discrete characters by reversible-jump Markov chain Monte Carlo. *American Naturalist*, **167**, 808-825.

Peakall R, Ruibal M, Lindenmayer DN (2003) Spatial autocorrelation analysis offers new insights into gene flow in the Australian bush rat, *Rattus fuscipes*. *Evolution*, **57**, 1182-1195.

Peakall R, Smouse PE (2006) GENALEX 6: genetic analysis in Excel. Population genetic software for teaching and research. *Molecular Ecology Notes*, **6**, 288-295.

R Development Core Team: R (2004) A language and environment for statistical computing. Vienna, Austria: R Foundation for Statistical Computing 2004.

Sehgal RNM, Buermann W, Harrigan RJ, Bonneaud C, Loiseau C, Chasar A, Sepil I, Valkiūnas G, Iezhova T, Saatchi S, Smith TB (2011) Spatially explicit predictions of blood parasites in a widely distributed African rainforest bird. *Proceeding of the Royal Society London B,* **278**, 1025-1033.

Figure S1.

Location of sampling sites in each of the three habitats; lowlands, highlands, and fynbos. Map created in ArcMap 10 (Environmental Systems Resource Institute, ArcMap 10.0 ESRI, Redlands, California).

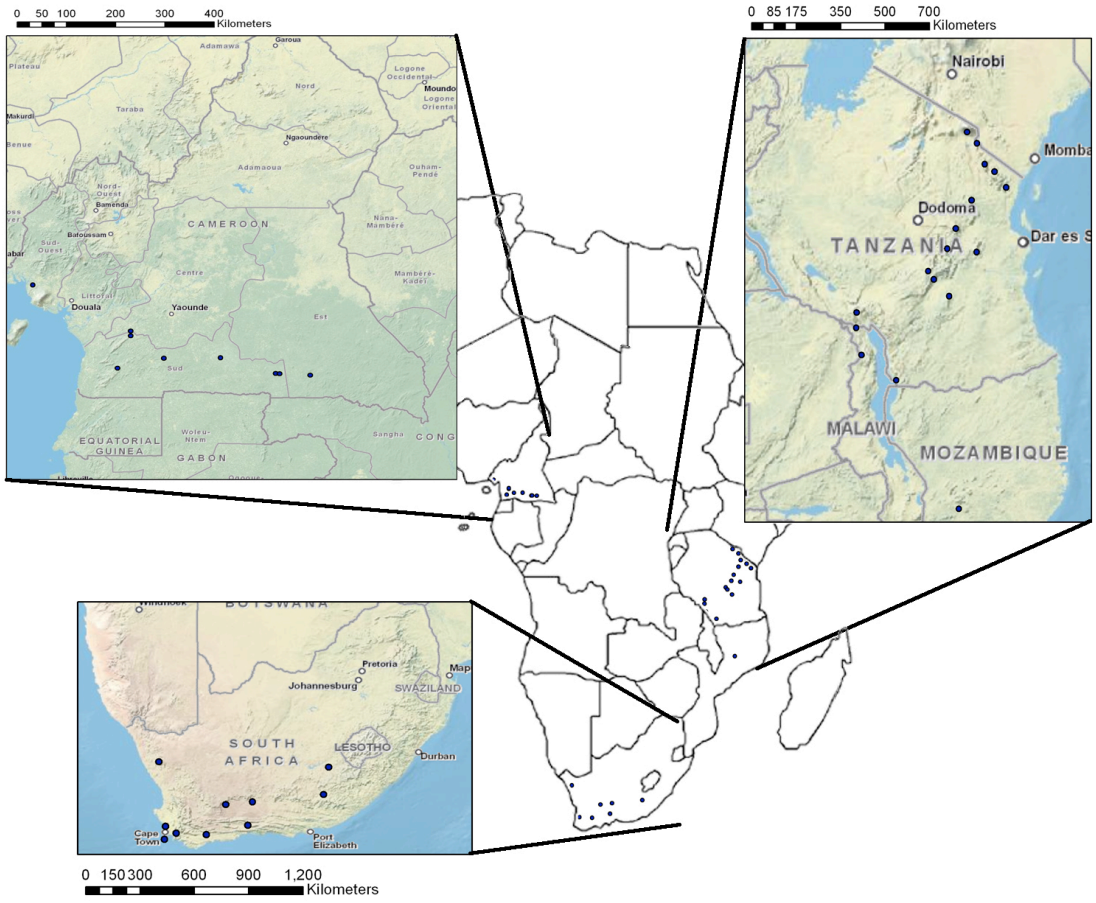

Figure S2.

Spatial autocorrelation in *Plasmodium* spp. prevalence in each of the three habitats; lowlands, highlands, and fynbos.

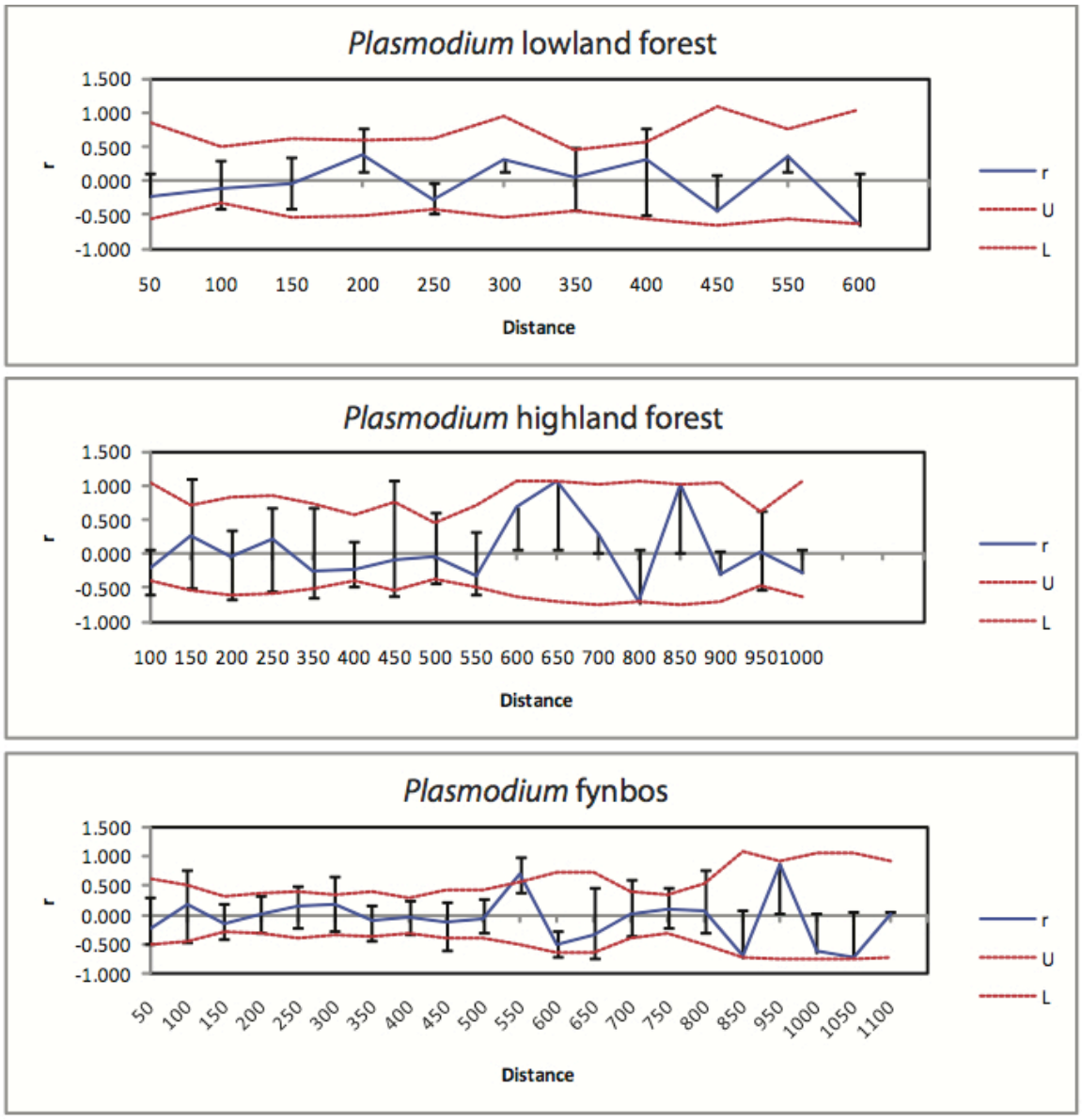

Table S1.
Coordinates and altitude at each sites (*) represents sites where *Plasmodium* infection was found.

Habitat	Site	Latitude	Longitude	Altitude (m)
Lowland	Ngoila (*)	N 2°37'39"	E 14°01'23.4"	528
	Zoebef (*)	N 2°39'31"	E 13°23'49"	601
	Bobo camp (*)	N 2°39'17"	E 13°28'16"	583
	CMNP North	N 2°46'07.1"	E 10°32'10.5"	485
	Douni (*)	N 2°58'11"	E 11°22'31.1"	722
	Mvono (*)	N 2°58'50.6"	E 12°24'09.5"	679
	Beh (*)	N 3°25'30"	E 10°46'36.3"	471
	Mvia (*)	N 3°31'03.2"	E 10°00'32.9"	48
	Mokoko (*)	N 4°27'23"	E 09°00'33"	127
Highland	Kilimanjaro (*)	S 03°13'	E 37°20'	1636
	North Pare	S 03°34'35"	E 37°40'20"	1622
	South Pare	S 04°16'00"	E 37°56'35"	2243
	West Usambara (*)	S 04°30'20"	E 38°16'05"	1837
	East Usambara (*)	S 05°02'00"	E 38°40'03"	1135
	Nguru (*)	S 05°27'00'	E 37°28'47"	1429
	Ukaguru	S 06°23'00"	E 36°56'20"	1942
	Rubeho (*)	S 07°03'00"	E 36°38'55"	1650
	Uluguru (*)	S 07°10'00"	E 37°40'00"	2445
	Udzungwa (*)	S 07°48'00"	E 36°00'00"	2014
	Livingstone (*)	S 08°04'00"	E 36°11'00"	489
	Mahenge (*)	S 08°37'00"	E 36°43'00"	588
	Rungwe	S 09°10'	E 33°32'	1356
	Misuku (*)	S 09°40'	E 33°31'	1415
	Nyika (*)	S 10°34'	E 33°42'	2187
	Matengo	S 11°24'	E 34°54'	475
	Namuli (*)	S 15°38'	E 37°03'	653
Fynbos	Aliwal North	S 30°39'24.12"	E 26°32'48.84"	1296
	Kamiesburg	S 30°22'23.88"	E 18°05'57.12"	1189
	Tarkastad	S 32°02'21.84"	E 26°17'35.88"	1352
	Beaufort West (*)	S 32°24'20.16"	E 22°45'46.08"	887
	Nova Vita	S 32°33'27"	E 21°25'58.80"	827
	De Rust	S 33°35'49.92"	E 22°31'36.84"	661
	Jonkershoek (*)	S 33°59'58"	E 18°57'38.14"	542
	Koeberg (*)	S 33°39'07.75"	E 18°26'19.51"	37
	Cape Peninsula (*)	S 34°18'34.58"	E 18°23'09.39"	10
	Bontebok NP (*)	S 34°04'40.08"	E 20°27'14.04"	64

Table S2.
Number of individual screened (N_{Total}) and number of infected individuals (N_{inf}) per host species. Diversity of *Plasmodium* lineages and number of birds found with a specific lineage (N) in the lowland rainforest.

Family	Species	N_{Total}	N_{inf}	Lineage	N
Muscicapidae	*Stiphornis erythrothorax*	14	6	PV8	6
Nectariniidae	*Cyanomitra olivaceus*	189	71	PV12	2
				PV13	8
				P-CYOL1	16
				PV16	6
				P-CYOL2	35
				PV19	2
				PV25a	1
				PV26	1
	Cinnyris chloropygius	57	14	P36	4
				PV12	3
				P-CYOL1	7
Pycnonotidae	*Andropadus latirostris*	230	59	PV1	22
				PV2	10
				PV3	14
				PV4	1
				PV6	1
				P-ANLA2	11
	Bleda notata	30	3	PV3	3
	Phyllastrephus icterinus	17	6	PV3	5
				PV4	1
Timaliidae	*Illadopsis rufipennis*	21	5	PV5	5
Turdidae	*Alethe diademata*	17	12	P-ALDI1	12

Table S3.
Number of individual screened (N_{Total}) and number of infected individuals (N_{inf}) per host species. Diversity of *Plasmodium* lineages and number of birds found with a specific lineage (N) in the highland rainforest.

Family	Species	N_{Total}	Ninf	Lineages	N
Muscicapidae	*Modulatrix stictigula*	40	9	PV12	5
				PV38	4
	Sheppardia sharpei	40	3	PV12	2
				PV38	1
Nectariniidae	*Cinnyris moreaui*	28	1	PV40	1
	Cinnyris usambaricus	29	0	-	
	Cinnyris fuelleborni	22	2	PV12	1
				PV25a	1
	Cinnyris whytei	12	1	P31	1
Platysteiridae	*Batis mixta*	39	3	PV12	1
				PV55	2
Pycnonotidae	*Andropadus chlorigula*	24	2	PV12	2
	Andropadus masukuensis	94	8	PV12	8
	Andropadus milanjensis	46	10	GRW6	1
				P26	1
				PV1	1
				PV12	7
Turdidae	*Alethe fuelleborni*	32	12	P15	1
				PV12	5
				P-ANLA1	1
				PV51	2
				WA15	3

Table S4.
Number of individual screened (N_{Total}) and number of infected individuals (N_{inf}) per host species. Diversity of *Plasmodium* lineages and number of birds found with a specific lineage (N) in the fynbos.

Family	Species	N_{Total}	Ninf	Lineage	N
Nectariniidae	*Cinnyris chalybeus*	41	8	P16	1
				PV25a	2
				PV41	5
	Nectarina famosa	85	13	P15	1
				P16	12
	Anthobaphes violacea	75	8	P16	5
				PV13	2
				PV41	1
Promeropidae	*Promerops cafer*	83	4	P15	1
				P16	2
				PV56	1
Pycnonotidae	*Pycnonotus capensis*	30	8	GRW11	3
				RFF1	1
				SGS1	4
Zosteropidae	*Zosterops capensis*	69	6	P15	6

Table S5.
Host specificity indices are given for each *Plasmodium* lineage found in each habitat.

Habitat	Lineage	Local S_{TD}	Global S_{TD}
Lowland	PV1	0.001	6.29
	PV2	0.001	0.001
	PV3	4	4.43
	PV4	2	2
	PV5	0.001	0.001
	PV6	0.001	0.001
	PV8	0.001	0.001
	P-ANLA2	0.001	0.001
	PV12	2	23.57
	PV13	0.001	16.57
	P-CYOL1	2	6
	PV16	0.001	3.46
	P-CYOL2	0.001	2
	PV19	0.001	0.001
	PV25a	0.001	8.57
	PV26	0.001	0.001
	P36	0.001	2
	P-ALDI1	0.001	4
Highland	PV1	0.001	6.29
	PV12	9.16	23.57
	P-ANLA1	0.001	5.16
	PV25a	0.001	8.57
	PV38	2	5
	PV40	0.001	4
	PV51	0.001	0.001
	PV55	0.001	0.001
	P15	0.001	18.43
	P26	0.001	4
	P31	0.001	9.21
	WA15	0.001	10.22
	GRW6	0.001	3.24
Fynbos	PV13	0.001	16.57
	PV25a	0.001	8.57
	PV41	0.001	3.46
	PV56	0.001	0.001
	P15	5	18.43
	P16	5.167	6.73
	GRW11	0.001	9.24
	RFF1	0.001	8.4
	SGS1	0.001	12.42

Table S6.
Distances (Km^2) between each site in the lowland West Africa habitat.

	Ngoila	Zoebef	Bobo camp	CMNP North	Douni	Mvono	Beh	Mvia	Mokoko
Ngoila	0	69.2	60.9	387.5	296.2	183.7	370.8	373.5	591.9
Zoebef	69.2	0	8.3	318.3	227.3	116.1	303.3	306.5	526.5
Bobo camp	60.9	8.3	0	326.6	235.6	124.1	311.3	314.2	534.1
CMNP North	387.5	318.3	326.6	0	95.6	208.6	77	86.7	252.2
Douni	296.2	227.3	235.6	95.6	0	114	83.4	89.9	310
Mvono	183.7	116.1	124.1	208.6	114	0	186.9	189.9	410.3
Beh	370.8	303.3	311.3	77	83.4	186.9	0	10.2	227
Mvia	373.5	306.5	314.2	86.7	89.9	189.9	10.2	0	222.5
Mokoko	591.9	526.5	534.1	252.2	310	410.3	227	222.5	0

Table S7.
Distances (Km^2) between each site in the highland East Africa habitat.

	Kilimanjaro	North Pare	South Pare	West Usambara	East Usambara	Nguru
Kilimanjaro	0	55.8	135.8	177.6	250.8	249.3
North Pare	55.8	0	83	123	196.1	209.4
South Pare	135.8	83	0	43.6	115.8	140.6
West Usambara	177.6	123	43.6	0	74.2	138
East Usambara	250.8	196.1	115.8	74.2	0	138.9
Nguru	249.3	209.4	140.6	138	138.9	0
Ukaguru	354.7	322	259.3	256.4	242.9	121.6
Rubeho	432.5	401.6	339.6	335.5	316	201.7
Uluguru	440.1	398.1	321.9	303.5	261.7	193.3
Udzungwa	529.8	503.5	446.2	444.2	425.4	309.4
Livingstone	553.1	524.3	463.2	458.2	434.1	325.3
Mahenge	602.9	568.4	499.7	487.8	452	362.6
Rungwe	782.6	770.2	729.2	736.2	728.4	600.9
Misuku	830.5	816.2	772.2	777.1	765.6	641.3
Nyika	908.3	889.8	839.7	840.4	821.7	704.8
Matengo	945.8	918.7	857.3	849.9	818.1	719.1
Namuli	1375.6	1336.4	1260.7	1239.8	1187.3	1129.8

	Ukaguru	Rubeho	Uluguru	Udzungwa	Livingstone	Mahenge	Rungwe	Misuku
Kilimanjaro	354.7	432.5	440.1	529.8	553.1	602.9	782.6	830.5
North Pare	322	401.6	398.1	503.5	524.3	568.4	770.2	816.2
South Pare	259.3	339.6	321.9	446.2	463.2	499.7	729.2	772.2
West Usambara	256.4	335.5	303.5	444.2	458.2	487.8	736.2	777.1
East Usambara	242.9	316	261.7	425.4	434.1	452	728.4	765.6
Nguru	121.6	201.7	193.3	309.4	325.3	362.6	600.9	641.3
Ukaguru	0	82.2	119.4	189.6	205.8	250.1	487	525.1
Rubeho	82.2	0	113.4	110.3	124.5	174.5	416.7	450.9
Uluguru	119.4	113.4	0	197.9	192.8	192.8	507.5	535.3
Udzungwa	189.6	110.3	197.9	0	36.7	120.7	311.8	343.5
Livingstone	205.8	124.5	192.8	36.7	0	84.9	315.6	342.2
Mahenge	250.1	174.5	192.8	120.7	84.9	0	355.7	370.6
Rungwe	487	416.7	507.5	311.8	315.6	355.7	0	57.1
Misuku	525.1	450.9	535.3	343.5	342.2	370.6	57.1	0
Nyika	585.8	507.2	577.2	398.1	388.1	395.2	157.5	102.3
Matengo	600.3	519	559.5	417.4	394.5	366.3	289.9	245.9
Namuli	1025.2	951.5	940	875.3	842.4	776.3	812.2	764.8

	Nyika	Matengo	Namuli
Kilimanjaro	908.3	945.8	1375.6
North Pare	889.8	918.7	1336.4
South Pare	839.7	857.3	1260.7
West Usambara	840.4	849.9	1239.8
East Usambara	821.7	818.1	1187.3
Nguru	704.8	719.1	1129.8
Ukaguru	585.8	600.3	1025.2
Rubeho	507.2	519	951.5
Uluguru	577.2	559.5	940
Udzungwa	398.1	417.4	875.3
Livingstone	388.1	394.5	842.4
Mahenge	395.2	366.3	776.3
Rungwe	157.5	289.9	812.2
Misuku	102.3	245.9	764.8
Nyika	0	160.7	668.6
Matengo	160.7	0	525.6
Namuli	668.6	525.6	0

Table S8.
Distances (Km^2) between each site in the fynbos in South Africa.

	Aliwal North	Kamiesburg	Tarkastad	Beaufort West	Nova Vita	De Rust
Aliwal North	0	811.3	155.2	408.3	529	500.1
Kamiesburg	811.3	0	802.2	497.5	398.8	550.3
Tarkastad	155.2	802.2	0	334.9	461	392.8
Beaufort West	408.3	497.5	334.9	0	125.9	133.5
Nova Vita	529	398.8	461	125.9	0	155.5
De Rust	500.1	550.3	392.8	133.5	155.5	0
Jonkershoek	804.4	410.2	718.5	395.7	280.3	332.4
Koeberg	833.5	365	756.4	426.6	304.3	378.5
Cape Peninsula	867.1	437.3	779	458.4	343.4	390
Bontebok NP	687.4	466.9	590.2	283.6	192.2	198.4

	Jonkershoek	Koeberg	Cape Peninsula	Bontebok NP
Aliwal North	804.4	833.5	867.1	687.4
Kamiesburg	410.2	365	437.3	466.9
Tarkastad	718.5	756.4	779	590.2
Beaufort West	395.7	426.6	458.4	283.6
Nova Vita	280.3	304.3	343.4	192.2
De Rust	332.4	378.5	390	198.4
Jonkershoek	0	60.4	62.9	139.2
Koeberg	60.4	0	73.3	192.4
Cape Peninsula	62.9	73.3	0	193.3
Bontebok NP	139.2	192.4	193.3	0